

Short communication

# Fabrication of patterned multi-walled poly-L-lactic acid conduits for nerve regeneration

Jianming Li<sup>a,c</sup>, Riyi Shi<sup>a,b,c,\*</sup>

<sup>a</sup> Weldon School of Biomedical Engineering, School of Veterinary Medicine, Purdue University, West Lafayette, IN 47907, United States

<sup>b</sup> Department of Basic Medical Sciences, School of Veterinary Medicine, Purdue University, West Lafayette, IN 47907, United States

<sup>c</sup> Center for Paralysis Research, School of Veterinary Medicine, Purdue University, West Lafayette, IN 47907, United States

Received 21 November 2006; received in revised form 3 June 2007; accepted 4 June 2007

## Abstract

Topographical cues in the micron and nanoscale regime represent a powerful and effective method for controlling neuron and glial cell behavior. Previous studies have shown that contact guidance can facilitate axon pathfinding, accelerate neurite growth and induce glial cell alignment. In this paper, we exploit the concept of haptotaxis via implementation into three-dimensional neural based scaffolds. Polymeric poly-L-lactic acid (PLLA) conduits possessing multiple intraluminal walls and precise topography along the longitudinal axis were fabricated using solvent casting, physical imprinting and a rolling-fusing method. Measurements made on scanning electron micrographs show the conduits demonstrate a transparency factor (void to polymer ratio) of up to 87.9% and an increase in surface area of four to eight times over comparably sized hollow conduits. Intraluminal wall thickness was approximately 20  $\mu\text{m}$  and physical parameters such as the number of lumens, conduit length and diameter were controllable. These results imply that the structures are conducive for cellular infiltration and proliferation. Although PLLA was used, the manufacturing techniques are highly flexible and are compatible with multiple polymer–solvent systems. Thus, the proposed conduits can be custom tailored to resorb in parallel with the healing process. Applications for these scaffolds include autograft substitutes for peripheral nerve transection or potential use in spinal cord related injuries.

© 2007 Elsevier B.V. All rights reserved.

**Keywords:** Topography; Nerve regeneration; Entubulation; Nerve scaffold

## 1. Introduction

In situations of peripheral nerve transection, end-to-end anastomosis is a preferred method for surgical intervention. However, in cases of large gap defects, anastomosis creates damaging tensile forces and autologous nerve grafts are required (Miyamoto, 1979; Maeda et al., 1999). Autologous grafts pose the problems of tissue availability, donor site morbidity, inconsistent functional outcome and neuroma formation (Mackinnon and Dellon, 1990). Consequently, multiple attempts have been made to manufacture bioartificial conduits that bridge the distal and proximal nerve stumps (Doolabh et al., 1996; Huang and Huang, 2006). Yet satisfactory functional outcome still remains elusive. It is well recognized that peripheral nerve regeneration across large

lesions is an incomplete process whereby cells do not receive the appropriate cues for successful reinnervation. Strategies that attempt to supplement the inherent biological deficiencies include the use of stimulatory electric fields/conducting substrates, contact guidance and relevant biochemical signals (Hudson et al., 1999; McCaig et al., 2005). However, no single element determines success but rather it is the synergistic effect between multiple cues that dictate cell fate and distal target reconnection. Therefore, a multi-faceted strategy that strives to mimic the natural *in vivo* environment is crucial for clinical success.

A first step in the combinatorial approach is the development of compatible scaffolds for delivery of desired stimuli. In this communication, we focus on integrating physical guidance as an initial phase of research. To this end, we have originated a method for fabricating neuro-compatible scaffolds with well-defined topography. Topographical information has relevance *in vivo* in the form of cell–cell and cell–matrix contact (Nordlander and Singer, 1982; Bunge, 1994). *In vitro*, neurons and glial cells can be directly oriented with surface patterning

\* Corresponding author at: Department of Medical Sciences, School of Veterinary Medicine, Purdue University, West Lafayette, IN 47907, United States. Tel.: +1 765 496 3018; fax: +1 765 494 7605.

E-mail address: riyi@purdue.edu (R. Shi).

techniques (Rajnicek et al., 1997; Miller et al., 2001). Translation of two-dimensional patterned surfaces into three-dimensional nerve guidance conduits, however, has proved to be challenging. The most difficult aspect of topography based nerve guides is the simultaneous control of topography with high void fraction (transparency factor). Incorporation of microchannels or longitudinal fibers along the length of the guides may prove feasible but the significant amount of bulk material traditionally required to fabricate these structures obstructs regenerating axons. We have circumvented some problems associated with previous iterations of multi-walled conduits by using solvent casting and conformal contact (embossing) techniques. The proposed method is unique in that it exploits the use of thin films as supporting wall structures. Not only do these conduits contain numerous internal surfaces, but the polymer walls are also physically etched with micron or nanometer sized features. The resultant increase in surface area coupled with a high transparency ratio provides more adhesion surfaces for cellular attachment. The physical guidance afforded by the wall patterns may also facilitate axon pathfinding, accelerate axonal outgrowth and minimize the risk of aberrant regeneration. The biodegradability of poly-L-lactic acid is another advantage as the host tissue will eventually replace the resident polymer. Biodegradation is also supportive of additional processing, such

as the incorporation of cytokines or pharmacological agents within the polymer matrix. Thus, a multi-stimuli method is attainable with the proposed neural scaffolds. Such scaffolds may prove promising for implementation in PNS grafting or even spinal cord repair.

## 2. Materials and methods

### 2.1. Preparation of polymer films

Patterned substrates were manufactured via a polymer casting and a stamping technique (Fig. 1, steps 1–4). Poly-L-lactide of inherent viscosity of 0.99–1.17 (Birmingham Polymers) was initially dissolved in chloroform in a 5% (w/v) concentration. Master templates used for polymeric patterning were obtained from several sources. Brushed stainless steel stock (McMaster-Carr) and holographic diffraction gratings (Edmunds Scientific, Optometrics) were used for the casting process. All templates were cleaned with a stream of compressed air and ethanol. Next, 2 mL of the PLLA solution was pipetted uniformly over a 10 cm × 10 cm portion of template. After 10 min of solvent evaporation (in fume hood), a secondary template was placed over the PLLA film, and aligned in the same direction as the casting master. Pressure was applied to the secondary template

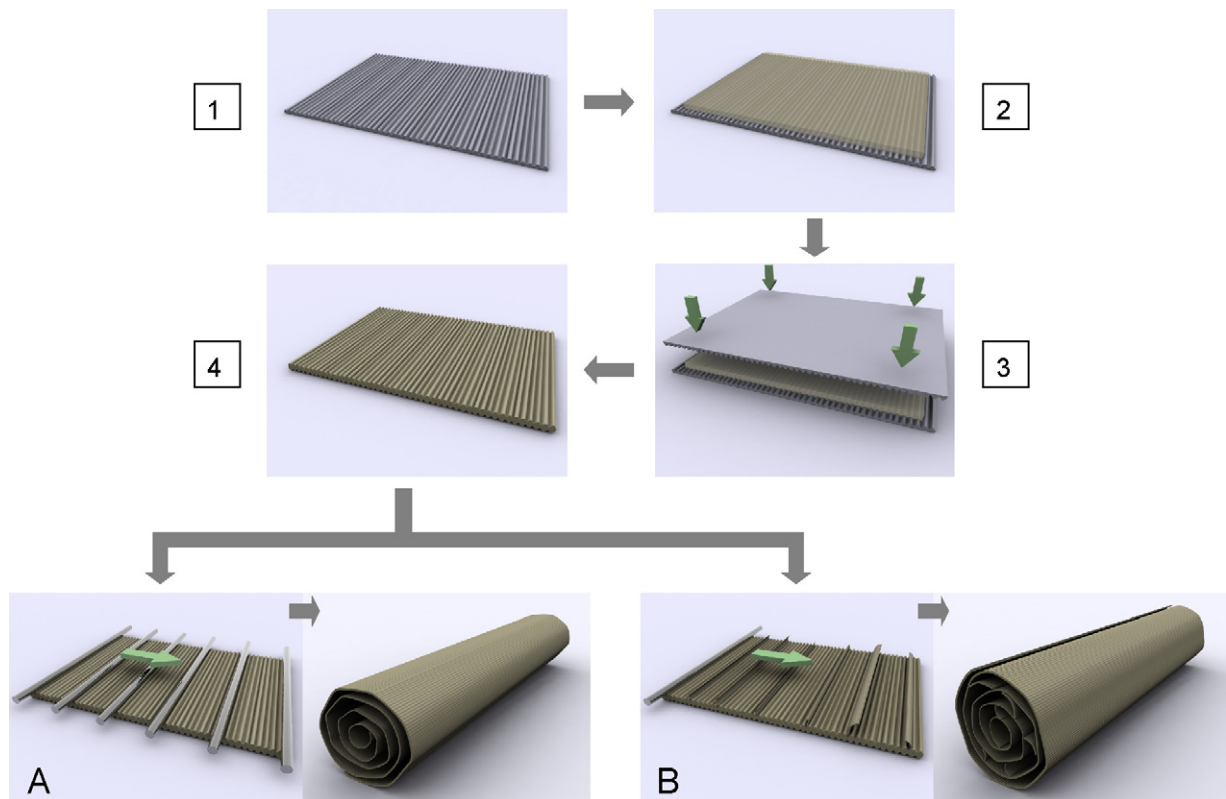


Fig. 1. Process for the manufacture of doubly patterned PLLA films and multi-walled conduits: (1) initial master template. (2) Solubilized PLLA is uniformly cast over the master template. The solvent is permitted to evaporate incompletely, leaving a compliant film. (3) A secondary template is aligned over the PLLA and through conformal contact, the top surface is imprinted. (4) The double-sided PLLA film is then peeled from the casting template and placed onto a glass surface. (A) Left: a stainless steel initiator wire is placed along an edge of the PLLA film and fixed in place with soluble PLLA solution. The wire is then rolled along the length of the PLLA sheet, using additional stainless steel wires as temporary spacers. Right: resultant PLLA conduit with spacers removed. (B) Left: an alternative assembly method using patterned PLLA strips as spacers and lumenal void filler. Right: finished conduit after rolling and fusing of free PLLA edge. Illustrations are not to scale.

to emboss the top surface. Following imprinting, the residual polymer and underlying master were cured in a fume hood for approximately 1 h. Then, the PLLA membrane was cut to size and carefully dissociated from the casting template. The polymer sheet was then utilized for conduit assembly.

## 2.2. Multi-walled polymer conduits

The partially cured PLLA polymer films were placed on a glass surface. A small stainless steel wire (127  $\mu\text{m}$  diameter) was placed along an edge of PLLA. Small droplets of dissolved PLLA solution was placed on this initiator wire near the edges of the film and allowed to solidify. This drop of frozen polymer fused the bottom PLLA film to the metal wire. For the rolling process, two methods were utilized to space the internal walls. Stainless steel wires (127  $\mu\text{m}$  diameter) and cut strips of patterned PLLA polymer were chosen as the wall spacing material (Fig. 1A and B). Either stainless steel spacing wires or PLLA filmstrips were then intermittently placed along the polymer sheet (for better reproducibility, the wires or strips could be fused with more PLLA solution to the parent polymer sheet at defined distances). The initiator wire was then carefully rolled down the remainder of the PLLA sheet. Once the PLLA sheet had been fully wound, a small swab of PLLA solution was brushed along the final edge, fusing the PLLA end to the wound roll. The PLLA cylinder was then cut at points between the fused joints. The central portion of the tube was kept, with the stainless steel initiator and spacing wires (if applicable) carefully removed. After drying, the PLLA was permanently cured by placement in a vacuum chamber at 25 inHg pressure for 48 h.

## 2.3. Atomic force microscopy (AFM) and scanning electron microscopy (SEM)

The topography of the PLLA polymer films were characterized using a PSIA XE-120 atomic force microscope. The measurements were made in tapping mode using a PSIA non-contact cantilever with a spring constant of 42 N/m and a nominal tip radius of 10 nm. The resonance frequency was 309 kHz. The original 256  $\times$  256 data point image fields were obtained at a scan rate of 1.0 Hz/line. All topography measurements were performed in air. AFM data was processed with XEI Software. For SEM, all polymer specimens were mounted onto aluminum disks and sputtered coated with gold–palladium. Imaging was performed on a JEOL JSM-840 SEM using a 5 kV acceleration voltage. Digital images were captured with 1280  $\times$  960 resolution and 160 s dwell time.

## 2.4. Geometric characterization

Fabricated PLLA conduits were characterized by several geometric parameters. First, two reference lines were drawn across the cross sectional SEM image. The lines corresponded to the widest and narrowest axes of the sectioned plane ( $d_1$ ,  $d_2$ ). These two values were averaged and the conduit diameter calculated. Internal lumen complexity was assessed by the number of wall intersections. This value was obtained by counting the number

of wall intersections when traversing two orthogonal reference lines. The enclosed area of the conduits was found by tracing the perimeter of the conduit and integrating the subsequent region. Average PLLA wall thickness was estimated by analysis of at least five locations throughout the conduit. To obtain the increase in surface due to the presence of internal walls, a surface area index (SAI) was devised. The SAI was defined as:

$$\text{Surface area index (SAI)} = \frac{\text{Total length of all wall edges}}{\text{Conduit perimeter}}$$

For instance, a hollow conduit with no internal walls would yield an SAI of 1.0. Note that in this formulation of SAI, the outer external surface of the conduit is included, the wall thickness is neglected and topography is ignored.

Finally, the cross sectional transparency factor was found. The transparency factor was defined as:

$$\% \text{Transparency} = \frac{A_{\text{total}} - A_{\text{polymer}}}{A_{\text{total}}} \times 100$$

where  $A_{\text{total}}$  is the total cross sectional area encompassed by conduit (bulk polymer + void) and  $A_{\text{polymer}}$  is the cross sectional area occupied by bulk polymer.

The transparency factor was measured by multiplying the measured average wall thickness and the total traced length of the wall edges. For image analysis, all micrographs were evaluated with Image Pro Plus Software.

## 3. Results

### 3.1. Image analysis

Solvent casting and stamping are highly flexible techniques and PLLA films with limitless topologies can be manufactured. In this study, topologies using three different source templates (holographic diffraction gratings, brushed stainless steel) were used. These templates were chosen based on the presence of unidirectional surface grooves. Atomic force microscopy (AFM) scans of replica PLLA from brushed stainless steel surfaces show a highly varied pattern (Fig. 2A). The surface features were predominately unidirectional but the undulations in height were relatively large. Ridge heights ranged from 0.2 to 0.8  $\mu\text{m}$  with irregular width spacing. In contrast, AFM data with diffraction gratings as master templates demonstrated more controllable and repeatable results (Fig. 2B–D). PLLA replica films containing 500, 1000, and 1200 lines/mm were lifted from the originals. Samples (500 lines/mm) possessed grooves of 250 nm in average height, while 1000 lines/mm specimens showed peak to valley groove heights averaging 125 nm. Spaced grooves (1200 lines/mm) showed ridge heights of only 60 nm.

### 3.2. Geometric and bulk feature analysis

Three-dimensional analysis of polymeric conduits were measured via SEM. Walled conduits were fabricated using two methods to space the intraluminal walls. Rolling the PLLA sheet with stainless steel spacers produced conduits with a spiral-like geometry (Fig. 3A). The spacing was controlled by the diam-

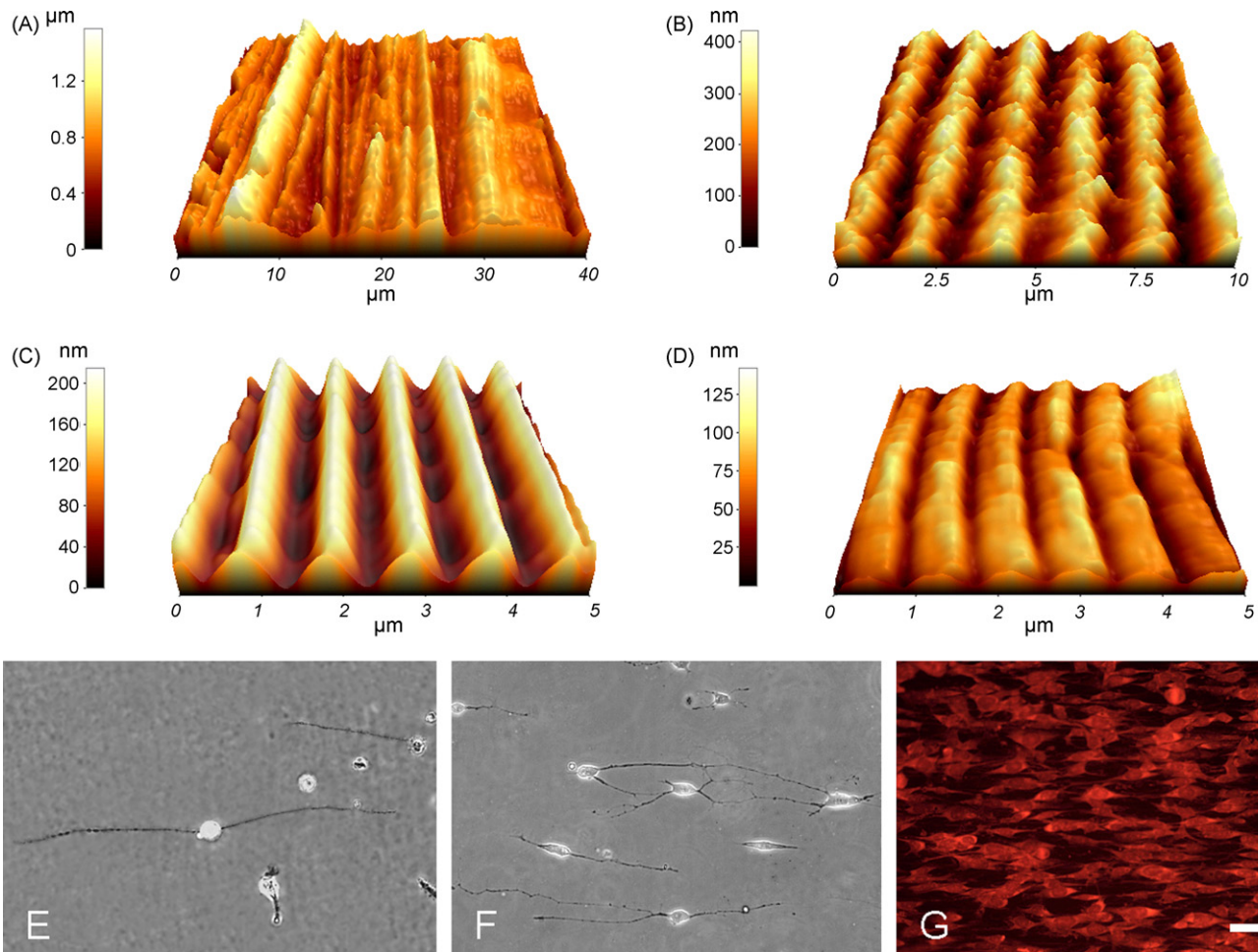


Fig. 2. Several different topologies were imprinted onto PLLA films. (A) Atomic force microscopy scans of replica PLLA from brushed stainless steel surfaces show a highly varied pattern. The surface ridges were predominately unidirectional but the undulations were relatively large. Ridge heights ranged from 0.2 to 0.8  $\mu\text{m}$  with irregular width spacing. In contrast, AFM data from diffraction grating based templates demonstrated more controllable and repeatable results. (B) Films with 500 lines/mm and average groove height of 250 nm. (C) PLLA replicas possessing 1000 lines/mm showed peak to valley heights averaging 125 nm, while (D) 1200 lines/mm spaced grooves showed ridge heights of only 60 nm. When dissociated neural and glial cells were cultured onto patterned PLLA of 1000 lines/mm (C), the cell behavior was well controlled. (E) After 24 h of incubation, chick dorsal root ganglia (DRG) neurons extended neurites along the direction of the grooves. (F) Chick sympathetic neurons also emanated processes parallel to the underlying pattern after 24 h. (G) A confluent Schwann cell monolayer that has been oriented along the PLLA ridge pattern. Schwann cells were fixed with 4% paraformaldehyde and stained with propidium iodide. Microscopy was performed with a Nikon Diaphot 200 using a 20 $\times$  objective. The images were captured with the PLLA grooves placed in the horizontal reference direction. Scale: 50  $\mu\text{m}$ .

eter of the wire spacers. When using patterned PLLA strips as wall spacers, the conduits were more irregular but compartmentalized. This latter production method resulted in conduits that more closely resemble natural fascicular structures (Fig. 3B). Oblique cuts on the conduit revealed distinct intraluminal walls (Fig. 3C and D). Higher magnification of the walls showed the bulk layers to be thin and non-porous (Fig. 3E). The films thickness ranged from 15 to 25  $\mu\text{m}$  and this fluctuation may have originated from uneven solvent evaporation/polymer accumulation or non-uniform surface flatness. However, we do not foresee these thickness variations to be significantly detrimental. The parallel micro/nano channels imprinted onto the film surfaces were clearly visible in the SEM (Fig. 3F).

Overall conduit properties showed some variation depending on the fabrication technique used. All conduit properties are reported in Fig. 4. As evident, the transparency factor was affected by film thickness, the number of layers and the gross

diameter of the conduit. The presence of multiple intraluminal walls also increased the available surface area for cell attachment. Using the SAI metric, the total surface area ranged from 3.83 to 6.62 times greater than comparably sized hollow conduits. Since topography also increases surface area, the SAI can be multiplied by a scalar quantity to achieve true changes in surface area. This scalar multiplier ( $k$ ) is topology specific and we report several values obtained from AFM analysis. Thus, the true change in surface area can range from approximately four to eight times greater than hollow conduits of the same perimeter.

When fully cured in the formed state, the PLLA conduits also possessed material elasticity (memory) and conduits would structurally rebound even after slight mechanical disturbance. This was demonstrated in Fig. 5 where an application of 0.2 N (or  $\sim 30\%$  nominal compression) for 1 min did not result in permanent deformation. Appropriate conduit sizing was achieved by cutting with surgical scissors (Fig. 6A).

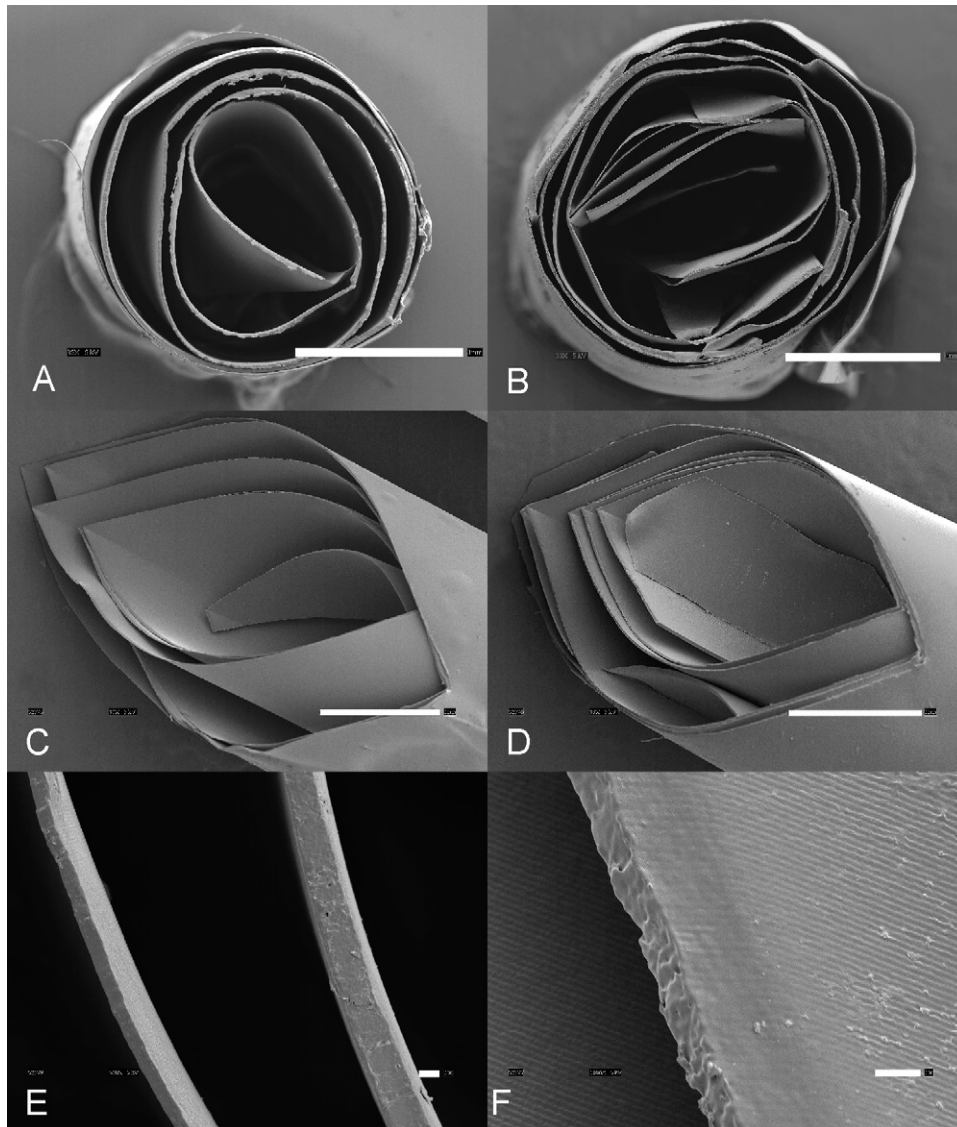


Fig. 3. (A) Scanning electron micrograph of a PLLA conduit cross section fabricated with stainless steel wires as intraluminal wall spacers. In this sample, the conduit enclosed an area of 2.80 mm<sup>2</sup> and had five wall layers. (B) SEM of PLLA conduit made with patterned PLLA strips as wall spacers and void filler. (C) An oblique section of a wire-rolled conduit, highlighting the multi-walled property. (D) A similarly angled slice of a strip impregnated conduit. (E) Higher magnification of the intraluminal side walls. (F) The intraluminal walls possessed highly controlled topography throughout the entire length of the conduit. In this sample, unidirectional grooves of 500 lines/mm and average peak to valley heights of 250 nm were imprinted. Scale: (A–D) 1 mm; (E and F) 10  $\mu$ m.

#### 4. Discussion

The entubulation method for severe PNS transection injuries yields promise as a viable alternative for autologous nerve grafts. Development of biocompatible and effective conduits would eliminate the associated autograft complications of donor site morbidity, graft geometry mismatch, neuroma formation and inconsistent performance (Mackinnon and Dellon, 1990). The literature is replete with innovative conduit designs and manufacturing protocols that strive to improve conduit performance. Approaches using endogenous biomaterials such as small intestinal submucosa, collagen, fibrin and acellularized nerve, muscle and vascular tissue have been utilized (Doolabh et al., 1996; Hudson et al., 1999; Hadlock et al., 2001; Haase et al.,

2003; Huang and Huang, 2006). Additionally, degradable and non-degradable materials including silicone, hydroxy-butyrates, polyesters, polyurethanes, chitosan and biocompatible hydrogels have also been researched (Doolabh et al., 1996; Hudson et al., 1999; Huang and Huang, 2006). Although natural biomaterials more closely mimic the structure–function relationship, the procedure of harvest and potential risks related to zoonotic disease and reliability can be problematic. Synthetic polymers offer the advantage of degradability or permanence, precise compositional control and capacity for timed drug/cytokine release. However, incorporating appropriate multiple stimuli and necessary biomechanical properties for successful outcome remains a challenge. Factors such as conduit geometry, biomaterial topography, internal matrix composition, cross sectional transparency

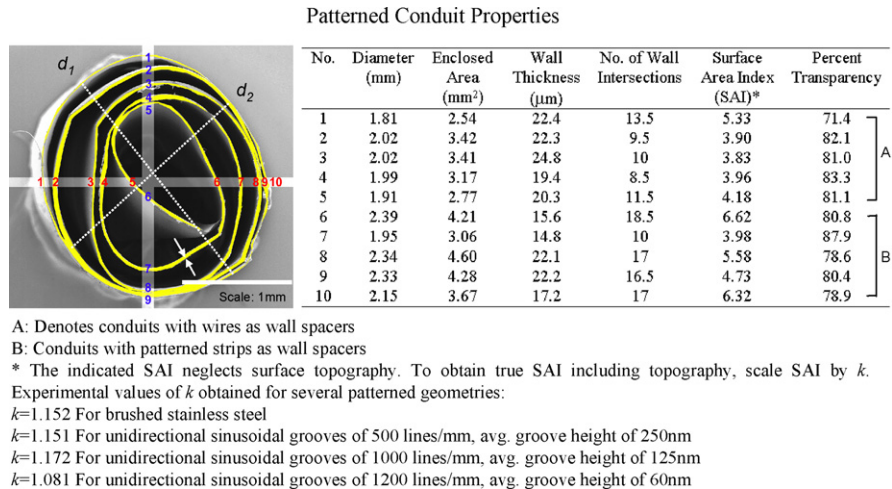


Fig. 4. Left: SEM of conduit cross section with key parameters superimposed. Wall thickness, average conduit diameter, number of wall intersections, and bulk polymer area are graphically shown. The number of wall intersections was found by counting the intersections between the orthogonal reference lines and the conduit walls (enumerated in horizontally and vertically). The bulk polymer face is masked and is used to convey the degree of transparency.  $d_1$  and  $d_2$  denote the major/minor axes used to estimate average conduit diameter. Right: complete table of all samples and their respective tabulated quantities.

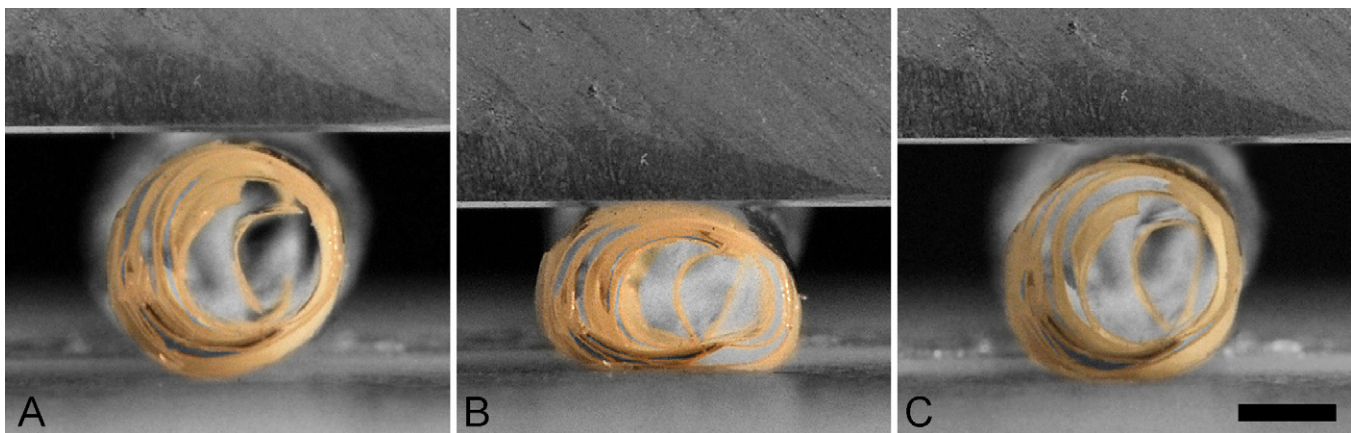


Fig. 5. PLLA conduits possessed elastic “memory” after complete cure in the formed state. This was demonstrated by compressing the PLLA conduits via a computerized load cell apparatus. (A) Image of the PLLA conduit prior to compression. (B) Image of the distorted conduit during brief (1 min) lateral compression. For this sample, the compression magnitude was  $\sim 30\%$  (0.2N applied force). (C) Following release of traction, the PLLA conduit rebounds to its original shape without noticeable permanent deformation or disruption of internal walls. Scale: 1 mm.

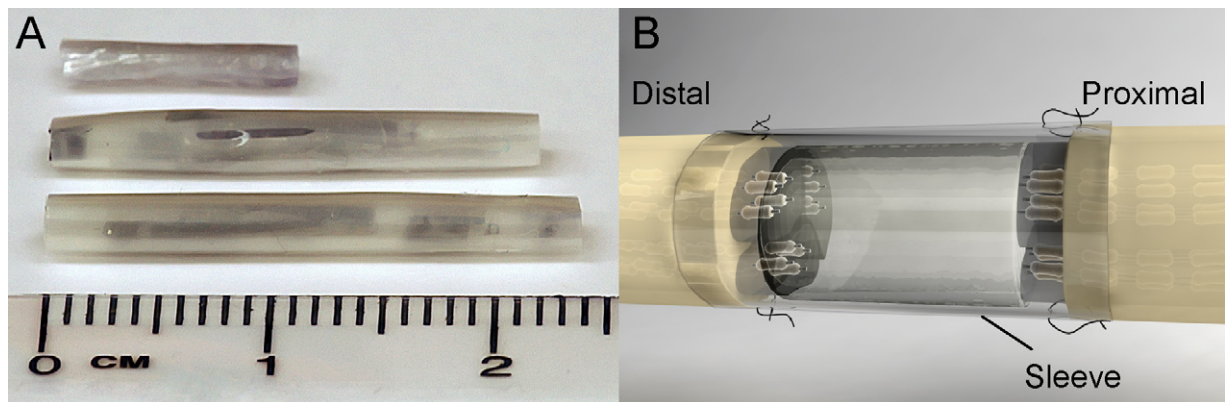


Fig. 6. (A) Images of several conduits manufactured by the rolling assembly technique. Conduits can vary from centimeters to millimeters in length and can be customized to the desired repair length. (B) The attachment scheme for *in vivo* implantation. Placement of the PLLA conduit within a sleeve, such as those fabricated from collagen may be clinically feasible. The collagen sleeve would serve as the containment unit and permit ease of suture across the lesion. Note that prior to placement within the supporting sleeve, pretreatment (such as protein coating, alterations to surface chemistry and sterilization) of the PLLA conduit should be executed.

factor, porosity/permeability, electrical conductivity and the presence of cytokines all play roles in dictating the degree of axonal regeneration (Hudson et al., 1999).

The manufacturing process of natural and polymer conduits have also varied and range from simple mandrel coating to more complicated procedures such as thermally induced phase separation, tissue acellularization, rolling-fusing assembly, lyophilization, fiber weaving, fiber filling and high strength magnetic field alignment (Fawcett and Keynes, 1986; Ceballos et al., 1999; Dubey et al., 2001; Ma and Zhang, 2001; Haase et al., 2003; Huang et al., 2005). In this paper, we report a relatively simple scheme for the fabrication of structurally stable polymer conduits comprising of multiple intraluminal walls and defined topography. The current method is unique to other techniques that address wall/bulk conduit properties but lack internal guidance structures (Evans et al., 1999; Young et al., 2002; Bini et al., 2004). The advantages of multi-walled patterned conduits for nerve regeneration are several-fold. First, the increase in surface area afforded by the internal walls and topography provides greater adsorption area for endogenous adhesion proteins. Secondly, the topographical cues provided by the continuous longitudinal patterns facilitate regeneration and axon pathfinding. Geometrically, the conduit partitions also mimic the natural fascicular anatomy and this property may also improve axonal bundle alignment while simultaneously reducing aberrant lateral excursions. Reducing aberrant regeneration is critical as misdirection is common in PNS injuries (Sumner, 1990).

The usage of thin films allowed us to achieve notable improvements over previous multi-lumen conduits. We were able to manufacture tubular structures with transparency values of up to 87.9% in conduits with diameters of less than 2 mm. A high void volume is vital as quality axonal regeneration is impossible if obstructed by parent material. This is evident as axonal outgrowth is affected by transparency factor even on a planar scale (Wallman et al., 2001). Increases in surface area from topography and internal walls ranged from four to eight times over comparably sized hollow conduits. Permeability for nutrient/gaseous exchange across wall partitions appears appropriate due to the relatively thin wall thickness ( $\sim 20 \mu\text{m}$ ). These collective results suggest the fabricated structures to be conducive for cellular infiltration and proliferation.

The reported assembly method permits great tolerance for unique structures. The parameters of thickness, diameter, layering complexity and topography are user-definable. Thickness can be altered by polymer–solvent concentration whereas the diameter, number of intraluminal walls and conduit length are dictated during assembly. The imparted topography is template dependent and can be fine-tuned based on *in vitro* cell studies. We found the inclusion of polymer spacers facilitated the assembly process and added an element of structural stability. This reinforcement should decrease the prospect of conduit collapse from *in vivo* forces. Furthermore, the parent biomaterial can be readily substituted and therefore, the conduits can be optimized to match the size, geometry and type of tissue defect. Attachment of the PLLA would be accomplished with an auxiliary sleeve (i.e. silicone, collagen) to assist proximal and distal stump suturing (Fig. 6B).

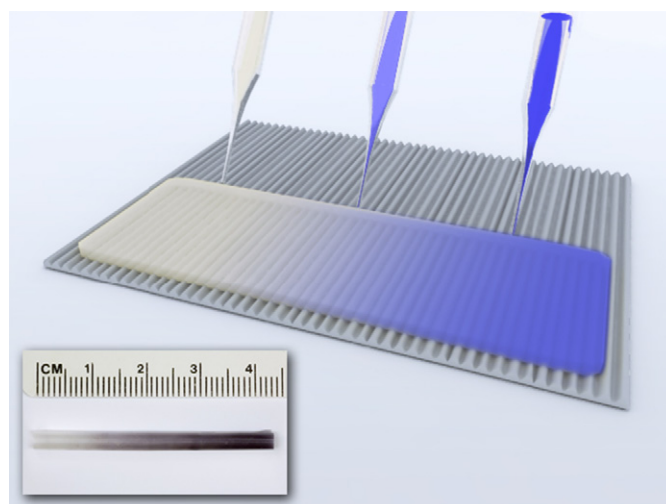


Fig. 7. Proof of concept for integration of biomolecules/pharmaceutics into the polymeric matrix. The solute of interest is dispersed within the polymer–solvent system. The individualized polymer solutions involve a progression of incrementally higher solute concentrations. During casting, the solutes mix and create a relatively smooth concentration gradient. The finalized films are subsequently assembled into multi-walled conduits. Inset: sample conduit with a concentration gradient embedded. The color gradient was generated by using a chloroform miscible dye.

We currently demonstrate a method for doubly imprinting PLLA surfaces with solvent casting and embossing, but the patterning approach is not limited to these two processes. Our technique produces highly controlled micro/nanotopography but equally viable alternatives include front and backside photolithography, adhesive peptide microcontact printing, or mechanical etching with ultra-fine grain sandpaper (Xia et al., 1999; Schmalenberg and Urich, 2005). Future additions to the multi-walled conduits include implementation of biologically active stimuli. For instance, patient harvested Schwann cells could be expanded *in vitro* and subsequently seeded into the conduit lumens (Komiyama et al., 2003). Schwann cells provide a physical substrate (via Bands of Bünger) for regeneration as well as secretion of supporting neurotrophic factors. Unoriented Schwann cell seeding can improve the degree of regeneration and we envision pre-seeding with oriented Schwann cells (aligned by the underlying substrate, see Fig. 2G) would further promote regeneration (Guenard et al., 1992; Hadlock et al., 2001). Similarly, the conduits can serve as a scaffold for other cells such as stem cells for CNS repair. Additional manipulations include timed release of neuron promoting agents such as NGF, BDNF, CNTF or inosine (Hadlock et al., 1999; Huang and Huang, 2006). The incorporation of such compounds can be accomplished during the initial solubilization process, where the biochemical or a pre-packaged form (i.e. loaded nanoparticles) can be dispersed within the polymer matrix (Tatard et al., 2005). Proof of this concept is shown in Fig. 7, in which a hydrophobic dye was used to create a concentration gradient across the length of the conduit. In a similar fashion, a homogeneous distribution or a gradient of neurotrophins can be integrated into the luminal walls.

## Acknowledgments

We would like to thank Michel Schweinsberg for his efforts with diagram illustrations and 3-D image renderings. This research was funded by the NSF Integrative Graduate Education and Research Training (IGERT) Program in Therapeutic and Diagnostic Devices DGE-99-72770 and the State of Indiana.

## References

- Bini TB, Gao S, Xu X, Wang S, Ramakrishna S, Leong KW. Peripheral nerve regeneration by microbraided poly(L-lactide-co-glycolide) biodegradable polymer fibers. *J Biomed Mater Res A* 2004;68:286–95.
- Bunge RP. The role of the Schwann cell in trophic support and regeneration. *J Neurol* 1994;242:S19–21.
- Ceballos D, Navarro X, Dubey N, Wendelschafer-Crabb G, Kennedy WR, Tranquillo RT. Magnetically aligned collagen gel filling a collagen nerve guide improves peripheral nerve regeneration. *Exp Neurol* 1999;158:290–300.
- Doolabh VB, Hertl MC, Mackinnon SE. The role of conduits in nerve repair: a review. *Rev Neurosci* 1996;7:47–84.
- Dubey N, Letourneau PC, Tranquillo RT. Neuronal contact guidance in magnetically aligned fibrin gels: effect of variation in gel mechano-structural properties. *Biomaterials* 2001;22:1065–75.
- Evans GR, Brandt K, Widmer MS, Lu L, Meszlenyi RK, Gupta PK, et al. In vivo evaluation of poly(L-lactic acid) porous conduits for peripheral nerve regeneration. *Biomaterials* 1999;20:1109–15.
- Fawcett JW, Keynes RJ. Muscle basal lamina: a new graft material for peripheral nerve repair. *J Neurosurg* 1986;65:354–63.
- Guenard V, Kleitman N, Morrissey TK, Bunge RP, Aebischer P. Syngeneic Schwann cells derived from adult nerves seeded in semipermeable guidance channels enhance peripheral nerve regeneration. *J Neurosci* 1992;12:3310–20.
- Haase SC, Rovak JM, Dennis RG, Kuzon Jr WM, Cederna PS. Recovery of muscle contractile function following nerve gap repair with chemically acellularized peripheral nerve grafts. *J Reconstr Microsurg* 2003;19:241–8.
- Hadlock T, Sundback C, Koka R, Hunter D, Cheney M, Vacanti J. A novel, biodegradable polymer conduit delivers neurotrophins and promotes nerve regeneration. *Laryngoscope* 1999;109:1412–6.
- Hadlock TA, Sundback CA, Hunter DA, Vacanti JP, Cheney ML. A new artificial nerve graft containing rolled Schwann cell monolayers. *Microsurgery* 2001;21:96–101.
- Huang YC, Huang YY. Biomaterials and strategies for nerve regeneration. *Artif Organs* 2006;30:514–22.
- Huang YC, Huang YY, Huang CC, Liu HC. Manufacture of porous polymer nerve conduits through a lyophilizing and wire-heating process. *J Biomed Mater Res B Appl Biomater* 2005;74:659–64.
- Hudson TW, Evans GR, Schmidt CE. Engineering strategies for peripheral nerve repair. *Clin Plast Surg* 1999;26:617–28, ix.
- Komiyama T, Nakao Y, Toyama Y, Asou H, Vacanti CA, Vacanti MP. A novel technique to isolate adult Schwann cells for an artificial nerve conduit. *J Neurosci Methods* 2003;122:195–200.
- Ma PX, Zhang R. Microtubular architecture of biodegradable polymer scaffolds. *J Biomed Mater Res* 2001;56:469–77.
- Mackinnon SE, Dellon AL. Clinical nerve reconstruction with a bioabsorbable polyglycolic acid tube. *Plast Reconstr Surg* 1990;85:419–24.
- Maeda T, Hori S, Sasaki S, Maruo S. Effects of tension at the site of coaptation on recovery of sciatic nerve function after neuroorrhaphy: evaluation by walking-track measurement, electrophysiology, histomorphometry, and electron probe X-ray microanalysis. *Microsurgery* 1999;19:200–7.
- McCaig CD, Rajniecek AM, Song B, Zhao M. Controlling cell behavior electrically: current views and future potential. *Physiol Rev* 2005;85:943–78.
- Miller C, Shanks H, Witt A, Rutkowski G, Mallapragada S. Oriented Schwann cell growth on micropatterned biodegradable polymer substrates. *Biomaterials* 2001;22:1263–9.
- Miyamoto Y. Experimental study of results of nerve suture under tension vs. nerve grafting. *Plast Reconstr Surg* 1979;64:540–9.
- Nordlander RH, Singer M. Spaces precede axons in Xenopus embryonic spinal cord. *Exp Neurol* 1982;75:221–8.
- Rajniecek A, Britland S, McCaig C. Contact guidance of CNS neurites on grooved quartz: influence of groove dimensions, neuronal age and cell type. *J Cell Sci* 1997;110(Pt 23):2905–13.
- Schmalenberg KE, Uehrich KE. Micropatterned polymer substrates control alignment of proliferating Schwann cells to direct neuronal regeneration. *Biomaterials* 2005;26:1423–30.
- Sumner AJ. Aberrant reinnervation. *Muscle Nerve* 1990;13:801–3.
- Tatard VM, Venier-Julienne MC, Saulnier P, Prechter E, Benoit JP, Menei P, et al. Pharmacologically active microcarriers: a tool for cell therapy. *Biomaterials* 2005;26:3727–37.
- Wallman L, Zhang Y, Laurell T, Danielsen N. The geometric design of micro-machined silicon sieve electrodes influences functional nerve regeneration. *Biomaterials* 2001;22:1187–93.
- Xia Y, Rogers JA, Paul KE, Whitesides GM. Unconventional methods for fabricating and patterning nanostructures. *Chem Rev* 1999;99:1823–48.
- Young RC, Wiberg M, Terenghi G. Poly-3-hydroxybutyrate (PHB): a resorbable conduit for long-gap repair in peripheral nerves. *Br J Plast Surg* 2002;55:235–40.